https://doi.org/10.1590/jatm.v17.1366 ORIGINAL PAPER

Application of the Unscented Kalman Filter for Tracking a Maneuvering Tank Modeled with a Second-Order Gauss-Markov Process: A Comparative Analysis with the Extended Kalman Filter

Hai Tran Van[1], *, Dien Nguyen Ngoc[1], Dung Pham Trung[1], Phon Nguyen Duy[2]

1.Le Quy Don Technical University – Institute of Missile and Control Engineering – Hanoi – Vietnam.
2.Le Quy Don Technical University – Department of Weapons – Hanoi – Vietnam.

***Corresponding author:** tranvanhai@lqdtu.edu.vn

ABSTRACT

This paper presents the application of the unscented Kalman filter (UKF) for estimating the dynamic states of a maneuvering tank using a second-order Gauss-Markov process model. The proposed method is effective in capturing the oscillatory characteristics, damping effects, and the impact of uncertain disturbances on the tank's dynamics, leading to improved estimation accuracy compared to traditional linear methods. Simulation results demonstrate that the UKF outperforms the extended Kalman filter (EKF) in accurately estimating the tank's position, velocity, and acceleration, even in the presence of significant noise and disturbances. This study highlights the superiority of the UKF in handling nonlinear dynamics and its potential application in military vehicle tracking systems.

Keywords: Nonlinear systems; Unscented Kalman filter; Second-order Gauss-Markov process; Maneuvering tank.

INTRODUCTION

Tracking maneuvering targets is a significant challenge due to the unavoidable inaccuracies in sensor systems and the lack of awareness regarding of unforeseen external forces that may act on the target, making it impossible to model the target's dynamic properties accurately. Today, there are many practical applications for tracking maneuvering targets using sensors such as sonar (Chen e*t al.* 2017), radar tracking (Zhai *et al.* 2018), and using radar and image sensor (Chen *et al.* 2015). A previous study Van *et al.* (2024) suggested a missile guidance law to improve anti-tank-guided missiles' performance against maneuvering tank targets. This guidance law assumes perfect knowledge of the target's state information, which is often unrealistic because tanks use complex maneuvers with unpredictable trajectories and variable acceleration. In addition, the guidance law proposed by Van *et al.* (2024) requires comprehensive information about the target's position, velocity, and acceleration. However, in practice, missile-integrated seekers usually measure only the target's position. Therefore, accurately estimating the target's position, velocity, and acceleration using modern filtering algorithms is crucial to providing the required input data for the missile guidance law.

Received: Sep. 07, 2024 | **Accepted:** Dec. 05, 2024
Peer review history: Single Blind Peer Review.
Section editor: Luiz Martins-Filho

Additionally, tanks often operate in harsh environments, facing complex challenges such as rough terrain, environmental disturbances, and unexpected forces. Therefore, accurately estimating the dynamic states of tanks in real-time becomes a significant challenge, requiring the application of advanced and highly effective estimation techniques.

Tracking maneuvering targets is challenging and has led to the development of various advanced algorithms. These include modeling unpredictable motions (Li and Jilkov 2003), optimizing filters such as the unscented Kalman filter (UKF), unscented particle filter, and cubature Kalman filter for nonlinear scenarios (Jagan *et al.* 2021; Rao and Babu 2008, Zhang *et al.* 2019), and using neural networks with multi-model approaches like the interacting multiple models for improved tracking (Ebrahimi *et al.* 2022; Visina *et al.* 2018). Combining these methods with machine learning enhances precision, especially for targets with complex, unpredictable movements (Sun *et al.* 2015).

Several studies have applied the extended Kalman filter (EKF) to solve the state estimation problem in nonlinear systems (Bellar 2019; Gite and Deodhar 2022; Kaur and Kaur 2016). However, EKF relies on linear approximations of nonlinear equations using a first-order Taylor expansion, which can lead to significant errors in highly nonlinear systems. The EKF requires the calculation of the Jacobian matrix for the state transition and measurement functions. This process can be complicated, especially for large nonlinear systems or those with complex structures. Calculating the Jacobian matrix is also prone to errors if these nonlinear functions have a complex form (Masooleh *et al.* 2022). In contrast, the UKF does not require linearization or Jacobian calculations, making it both simpler and more accurate for nonlinear systems. The UKF uses sigma points to approximate probability distributions, enhancing its ability to handle sudden changes and complex noise. As a result, the UKF is generally more effective than the EKF in applications involving high nonlinearity and complex environments (Wan and Merwe 2000).

However, existing research has not explored the use of optimal filters for tracking military vehicles or maneuvering tanks. Visina *et al.* (2018) presented advanced filtering algorithms designed to track moving targets with aggressive maneuvers. It introduces a novel model that detects sharp turns quickly by employing a turn-rate white noise model with a non-zero mean, distinguishing it from traditional Wiener models. Nonetheless, the application of advanced filters, such as the UKF and its variants, for tracking maneuvering tanks on the ground using a second-order Gauss-Markov process seems to be insufficiently investigated or not thoroughly explored in the current literature.

However, current UKF research mainly focuses on civilian vehicles (Ponsa *et al.* 2005), and no studies have applied it to the state estimation of tank motion. To fully capture the complex dynamics of tanks, including damping, natural frequency, and unpredictable disturbances from unknown forces, a more accurate model is needed to illustrate tank movement.

To address these limitations, the present study proposes the use of a second-order Gauss-Markov model to describe tank dynamics combined with the UKF to estimate the tank's state as it moves along the x-axis. This second-order Gauss-Markov model is more detailed and provides a better simulation of the dynamic factors of the tank, including damping effects, natural frequency, and inertial delays. As a result, the model more accurately reflects the real behavior of tanks in combat environments, especially when facing unpredictable disturbances and forces. The tank's movement model along the x-axis ensures simplicity while remaining practical, representing the typical behavior of maneuverable combat vehicles like tanks. This research contributes to applying advanced estimation techniques for combat vehicles in military environments.

Tank dynamic mathematical model

Tank motion model in the horizontal plane

Since the tank's motion is confined to ground movements (forward, backward, and lateral), the coordinate system used in the two-dimensional horizontal plane model is illustrated in Fig. 1. In the Cartesian coordinate system, tank motion can be divided into two main components: alongtrack acceleration and crosstrack acceleration. Accelerations in the non-rotating Cartesian reference frame can be expressed as Sreeja and Hablani (2016).

$$\ddot{x}_t = a_{Tx}\sin\theta + a_{Tz}\cos\theta = a_{Tx}(\dot{x}_t/V_T) + a_{Tz}(\dot{z}_t/V_T) \tag{1}$$

$$\ddot{z}_t = a_{Tx}\cos\theta - a_{Tz}\sin\theta = a_{Tx}(\dot{z}_t/V_T) - a_{Tz}(\dot{x}_t/V_T) \tag{2}$$

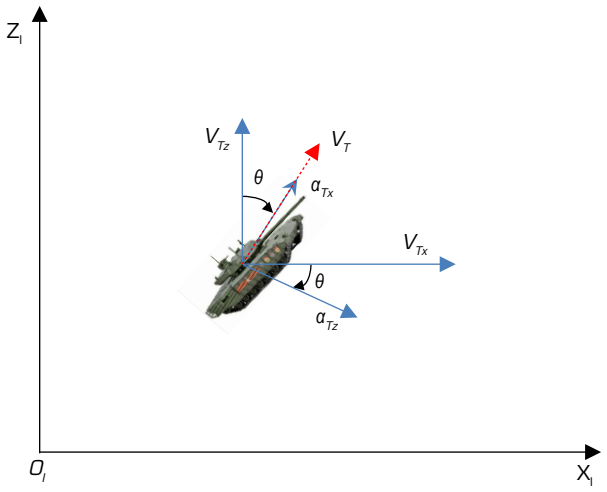

Source: Elaborated by the authors.

Figure 1. The ground horizontal plane coordinate system of the tank.

In this context, the acceleration components a_{Tx} and a_{Tz} of the tank are determined along the x and z-axes of the tank's body. These components are modeled using a Gauss-Markov process, which can be either first-order or second-order, with parameters selected based on the results from anti-tank missile tests (Gibbs 2011). The angle θ represents the direction of the target's velocity. For evasive maneuvers, the tank's heading angle θ is measured relative to the z-axis, as illustrated. The tank's velocity V_T moves in the direction specified by θ, with a_{Tx} being the acceleration along this direction and being the acceleration in the perpendicular direction. Therefore, when the tank moves along the x-axis, the angle θ will be 90 degrees.

The dynamics of the maneuvering tank are modeled using a second-order Gauss-Markov process, which provideds a more accurate representation of the tank's acceleration. This model in the paper specifically focuses on the tank's behavior along the x-axis within the horizontal plane, corresponding to the munition's trajectory plane.

The dynamic model of the tank using a second-order Gauss-Markov process

This study focuses on the alongtrack acceleration, representing the tank's movement along the x-axis. This acceleration is modeled using a second-order Gauss-Markov process, which effectively captures the oscillatory behavior of the tank's dynamics. Accordingly, the accelerations are characterized by Markov processes with transfer functions, as described by the following equation (Gibbs 2011; Sreeja and Hablani 2016).

$$H(s) = \frac{s + \frac{1}{\tau}}{s^2 + 2\zeta\omega_n s + \omega_n^2} \tag{3}$$

Using the inverse Laplace transform method, the transfer function can be converted from the frequency domain to the continuous time domain. In this case, the tank's dynamic model along the x-axis can be described by a second-order Gauss-Markov model, with the continuous differential equation for acceleration a_{Tx} expressed as follows:

$$\ddot{a}_{Tx}(t) + 2\zeta\omega_n \dot{a}_{Tx}(t) + \omega_n^2 a_{Tx}(t) = \dot{W}(t) + \frac{1}{\tau} W(t) \tag{4}$$

where a_{Tx} is the tank's acceleration at time, W is the input noise at time, ζ is the damping coefficient, describing the degree of oscillation damping in the system, ω_n is the natural frequency, determining the natural oscillation rate of the system, and τ is the time constant, describing the system's delay.

This differential equation indicates that the tank's acceleration is influenced not only by its current state but also by input noise and dynamic parameters such as damping and natural frequency. The second-order Gauss-Markov process captures the

relationship between successive acceleration states, enabling an accurate modeling of the tank's dynamic response to forces and disturbances in combat environments. The general solution of the differential Eq. 4 is:

$$a_{Tx}(t) = a_{Tx,h}(t) + a_{Tx,p}(t) \tag{5}$$

Here, $a_{Tx,h}(t)$ is the homogeneous solution and $a_{Tx,p}(t)$ is the particular solution. The homogeneous solution of a second-order differential equation in the continuous time domain, obtained by setting the right-hand side of the Eq. 4 to zero, is:

$$a_{Tx,h}(t) = e^{-\zeta\omega_n t}\left(C_1\cos(\omega_d t) + C_2\sin(\omega_d t)\right) \tag{6}$$

where $\omega_d = \omega_n\sqrt{1-\zeta^2}$ is the damped natural frequency and C_1 and C_2 are constants determined by the initial conditions.

The derivative of the homogeneous solution in the continuous time domain is:

$$\dot{a}_{Tx,h}(t) = e^{-\zeta\omega_n t}\left[-\zeta\omega_n\left(C_1\cos(\omega_d t) + C_2\sin(\omega_d t)\right) - \omega_d C_1\sin(\omega_d t) + \omega_d C_2\cos(\omega_d t)\right] \tag{7}$$

Discretizing the time domain into steps $t=k\Delta t$, the solution at time step k is:

$$a_{Tx,h}[k] = e^{-\zeta\omega_n k\Delta t}\left(C_1\cos(\omega_d k\Delta t) + C_2\sin(\omega_d k\Delta t)\right) \tag{8}$$

At time step $k-1$:

$$a_{Tx,h}[k-1] = e^{-\zeta\omega_n (k-1)\Delta t}\left(C_1\cos(\omega_d (k-1)\Delta t) + C_2\sin(\omega_d (k-1)\Delta t)\right) \tag{9}$$

The relationship between $a_{Tx,h}[k]$ and $a_{Tx,h}[k-1]$ is derived using exponential properties to relate successive terms via $e^{-\zeta\omega_n k\Delta t}$, trigonometric identities to simplify cosine and sine terms for adjacent steps, discretization to evaluate the continuous solution at $t = k\Delta t$ and $t = (k-1)\Delta t$, and linear combination to incorporate terms from the solution and its derivative at step $k-1$.

$$a_{Tx,h}[k] = e^{-\zeta\omega_n\Delta t}\begin{pmatrix} a_{Tx,h}[k-1]\cos(\omega_d\Delta t) + \\ e^{-\zeta\omega_n (k-1)\Delta t}(C_2\cos(\omega_d (k-1)\Delta t) - C_1\sin(\omega_d (k-1)\Delta t))\sin(\omega_d\Delta t) \end{pmatrix} \tag{10}$$

Applying Eq. 7 to the discrete-time domain at $t = (k-1)\Delta t$, the derivative of the homogeneous solution at step $k-1$ is:

$$\begin{aligned} \dot{a}_{Tx,h}[k-1] = e^{-\zeta\omega_n (k-1)\Delta t}\Big[&-\zeta\omega_n\left(C_1\cos(\omega_d (k-1)\Delta t) + C_2\sin(\omega_d (k-1)\Delta t)\right) \\ &-C_1\omega_d\sin(\omega_d (k-1)\Delta t) + C_2\omega_d\cos(\omega_d (k-1)\Delta t)\Big] \end{aligned} \tag{11}$$

Using the expression from Eq. 9 in Eq. 11, $\dot{a}_{Tx,h}[k-1]$ is expressed as follows:

$$\dot{a}_{Tx,h}[k-1] = -\zeta\omega_n a_{Tx,h}[k-1] + \omega_d e^{-\zeta\omega_n (k-1)\Delta t}(-C_1\sin(\omega_d (k-1)\Delta t) + C_2\cos(\omega_d (k-1)\Delta t)) \tag{12}$$

Since the target's acceleration is relatively small, the term $\dot{a}_{Tx,h}[k-1]$ can be neglected to simplify the expression. From Eq. 12, we have:

$$e^{-\zeta\omega_n (k-1)\Delta t}(-C_1\sin(\omega_d (k-1)\Delta t) + C_2\cos(\omega_d (k-1)\Delta t)) \approx \frac{\zeta\omega_n a_{Tx,h}[k-1]}{\omega_d} \tag{13}$$

Substituting Eq. 13 into the expression for $a_{Tx,h}[k]$, we have:

$$a_{Tx,h}[k] \triangleq e^{-\zeta\omega_n\Delta t}\left(a_{Tx,h}[k-1]\cos(\omega_d\Delta t)+\frac{\zeta\omega_n}{\omega_d}a_{Tx,h}[k-1]\sin(\omega_d\Delta t)\right) \tag{14}$$

The formula for the homogeneous solution $a_{Tx,h}[k]$ provides a comprehensive description of the state of a second-order oscillatory system in discrete space, capturing key dynamic behaviors. It describes periodic oscillations with the frequency ω_d, the effect of energy decay through the damping factor $e^{-\zeta\omega_n\Delta t}$, and the dependency on the previous state $a_{Tx,h}[k-1]$.

Since $\dot{W}(t)$ is the derivative of white noise, it remains a random process. To simplify the problem, we can assume the right-hand side of the Eq. 4 is $W(t)$, white noise with variance σ_w^2. To derive the particular solution $a_{Tx,p}(t)$, the following mathematical techniques are utilized. First, the Green's function method is applied to represent the response of the second-order oscillatory system to the input noise $W(t)$ in the continuous time domain. The Green's function, given by $G(t)=\frac{1}{\omega_d}e^{-\zeta\omega_n t}\sin(\omega_d t)$, is used to convolve with the noise $W(t)$, forming the continuous particular solution:

$$a_{Tx,p}(t)=\int_0^t G(t-\tau)W(\tau)d\tau \tag{15}$$

Next, the discrete-time domain transformation technique is applied, where the continuous domain is sampled at discrete points $t=k\Delta t$. The Green's function in the discrete domain is expressed as:

$$G[k]=\frac{1}{\omega_d}e^{-\zeta\omega_n k\Delta t}\sin(\omega_d k\Delta t) \tag{16}$$

The convolution in the continuous domain is replaced by a discrete summation:

$$a_{Tx,p}[k]=\sum_{i=0}^{k}G[k-i]W[i]\Delta t \tag{17}$$

Subsequently, the statistical properties of white noise $W[k]$ are employed, where $\mathsf{E}[W[k]]=0$ and $\mathsf{E}[W[k]^2]=\sigma_w^2$, to simplify the energy of the signal passing through the Green's function. Energy analysis indicates that the white noise decays with a factor $e^{-\zeta\omega_n k\Delta t}$ determined by the system's dynamic parameters. Finally, the energy approximation technique is applied, resulting in the simplified form of the particular solution:

$$a_{Tx,p}[k]\approx\sigma_w\sqrt{1-e^{-2\zeta\omega_n\Delta t}}\eta_k \tag{18}$$

where $\eta[k]$ is a normalized random variable, i.e., $\eta_k \sim \mathsf{N}(0,1)$, with a mean of 0 and a variance of 1.

Combining Eqs. 14 and 18, we obtain the expression representing the tank's acceleration in the discrete domain as follows:

$$a_{Tx}[k] \triangleq e^{-\zeta\omega_n\Delta t}\left(a_{Tx}[k-1]\cos(\omega_d\Delta t)+\frac{\zeta\omega_n}{\omega_d}a_{Tx}[k-1]\sin(\omega_d\Delta t)\right)+\sigma_w\sqrt{1-e^{-2\zeta\omega_n\Delta t}}\eta_k \tag{19}$$

Nonlinear state transition function and measurement function

The nonlinear state transition function for the system is crucial for capturing the dynamics of a maneuvering tank, which are influenced by complex physical forces. The tank's acceleration a_{Tx} at each discrete time step is modeled by a second-order Gauss-Markov process, accounting for the natural damping and oscillatory behavior of the system. The state vector $\mathbf{x}_k$ at time step k includes the position x_k, velocity $\dot{x}_k$, and acceleration $\ddot{x}_k$ along the x-axis. The state transition function $\boldsymbol{f}(\boldsymbol{x}_k,\boldsymbol{w}_k)$ describes how these states evolve over time, influenced by the previous states and the process noise $\mathbf{w}_k$.

The position x_{k+1} at time step $k+1$ is given by:

$$x_{k+1}=x_k+\dot{x}_k\cdot\Delta t+0.5\cdot\ddot{x}_k\cdot\Delta t^2 \tag{20}$$

The velocity $\dot{x}_{k+1}$ at time step $k+1$ is given by:

$$\dot{x}_{k+1} = \dot{x}_k + \ddot{x}_k \cdot \Delta t \tag{21}$$

The acceleration $\ddot{x}_{k+1}$ at time step $k+1$ is given by:

$$\ddot{x}_{k+1} = e^{-\zeta\omega_n \Delta t}\left(\cos(\omega_d \Delta t) + \frac{\zeta\omega_n}{\omega_d}\sin(\omega_d \Delta t)\right)\ddot{x}_k + \sigma_w\sqrt{1-e^{-2\zeta\omega_n \Delta t}}\,\eta_k \tag{22}$$

The discrete-time state transition equation for the system is given by:

$$\mathbf{x}_{k+1} = A\mathbf{x}_k + \mathbf{w}_k \tag{23}$$

From Eq. 20 to Eq.23, the state transition matrix A is defined as:

$$A = \begin{bmatrix} 1 & \Delta t & 0.5\cdot\Delta t^2 \\ 0 & 1 & \Delta t \\ 0 & 0 & e^{-\zeta\omega_n \Delta t}\left(\cos(\omega_d \Delta t) + \frac{\zeta\omega_n}{\omega_d}\sin(\omega_d \Delta t)\right) \end{bmatrix} \tag{24}$$

In this matrix, the first row updates the position x_k based on the current velocity $\dot{x}_k$ and acceleration $\ddot{x}_k$, the second row updates the velocity $\dot{x}_k$ considering the current acceleration $\ddot{x}_k$, the third row represents the evolution of the acceleration $\ddot{x}_k$ at the next time step, is also governed by the constants: time constant τ, damping coefficient ζ, natural frequency ω_n, and time step Δt.

The process noise $\mathbf{w}_k$ is defined as:

$$\mathbf{w}_k = \begin{bmatrix} 0 \\ 0 \\ \sigma_w\sqrt{1-e^{-2\zeta\omega_n \Delta t}}\,\eta_k \end{bmatrix} \tag{25}$$

$\mathbf{w}_k$ represents the external process noise affecting the acceleration, with a standard deviation σ_w, indicating the system's random oscillations. The noise intensity is also influenced by the constants: time constant τ, damping coefficient ζ, natural frequency ω_n, and time step Δt.

The measurement function $\boldsymbol{h}(\boldsymbol{x}_k, \boldsymbol{v}_k)$ relates the system's state to the observed measurements. For this system, where only the position x_k is measured, the function is given by:

$$\boldsymbol{z}_k = \boldsymbol{h}(\boldsymbol{x}_k) + \boldsymbol{v}_k = \begin{bmatrix} 1 & 0 & 0 \end{bmatrix}\boldsymbol{x}_k + \boldsymbol{v}_k \tag{26}$$

where $\mathbf{z}_k$ is the measurement vector at time step k and $\mathbf{v}_k$ is the measurement noise, which is assumed to be Gaussian with zero mean and covariance $\mathbf{R}$.

This function maps the state vector to the measured output, specifically focusing on the position x_k, while accounting for measurement noise. Together, the state transition and measurement functions provide the foundation for estimating the tank's state in a discrete-time nonlinear system, enabling accurate tracking and prediction. The random variables $\mathbf{w}_k$ and $\boldsymbol{v}_k$ are assumed to be process noise and measurement noise, respectively, independent of each other, white noise in nature, and normally distributed

with zero mean and specified variance: $w_k \sim \mathrm{N}(0, Q)$ and $v_k \sim \mathrm{N}(0, R)$, with $E\left(w_i,\ v_j\right) = 0$. These are fundamental assumptions in Kalman filter theory, ensuring the effectiveness of estimates when applied to systems with random noise.

Application of Kalman filters for target state estimation

This section examines the specific filtering techniques used to estimate the state of the maneuvering tank, focusing on the EKF and UKF. The core principles and implementation details of each filter are discussed, building on the state transition and measurement models described in the section "Nonlinear state transition function and measurement function".

Application of the EKF

The EKF is an extension of the classical Kalman filter, tailored to handle the nonlinearities in the state transition and measurement functions. It approximates these nonlinearities by linearizing the functions around the current estimate using a first-order Taylor expansion.

Linearization

The EKF linearizes the nonlinear state transition function $\boldsymbol{f}(\boldsymbol{x}_k, \boldsymbol{w}_k)$ and measurement function $\boldsymbol{h}(\boldsymbol{x}_k)$ described in the section "Nonlinear state transition function and measurement function". Linearization is performed by computing the Jacobian matrices at each time step:

$$\boldsymbol{F}_k = \frac{\partial \boldsymbol{f}(\boldsymbol{x}_k)}{\partial \boldsymbol{x}_k}\Big|_{\hat{\boldsymbol{x}}_k} \tag{27}$$

$$\boldsymbol{H}_k = \frac{\partial \boldsymbol{h}(\boldsymbol{x}_k)}{\partial \boldsymbol{x}_k}\Big|_{\hat{\boldsymbol{x}}_k} \tag{28}$$

where $\mathbf{F}_k$ is the Jacobian of the state transition function and $\mathbf{H}_k$ is the Jacobian of the measurement function. These matrices represent the linear approximations of the system around the current state estimate.

EKF algorithm

The EKF algorithm proceeds in two main steps: prediction and update.

Prediction step

Using the linearized model, the predicted state and covariance are calculated as:

$$\hat{\boldsymbol{x}}_{k+1|k} = \boldsymbol{f}(\hat{\boldsymbol{x}}_k) \tag{29}$$

$$\mathbf{P}_{k+1|k} = \mathbf{F}_k \mathbf{P}_k \mathbf{F}_k^{\bullet} + \mathbf{Q} \tag{30}$$

Update step

The Kalman gain, updated state estimate, and updated error covariance are computed as follows:

$$\mathbf{K}_k = \mathbf{P}_{k+1|k} \mathbf{H}_k^{\bullet} \left(\mathbf{H}_k \mathbf{P}_{k+1|k} \mathbf{H}_k^{\bullet} + \mathbf{R}\right)^{-1} \tag{31}$$

$$\hat{\boldsymbol{x}}_{k+1} = \hat{\boldsymbol{x}}_{k+1|k} + \boldsymbol{K}_k \left(\boldsymbol{z}_k - \boldsymbol{h}(\hat{\boldsymbol{x}}_{k+1|k})\right) \tag{32}$$

$$\mathbf{P}_{k+1} = \left(\mathbf{I} - \mathbf{K}_k \mathbf{H}_k\right) \mathbf{P}_{k+1|k} \tag{33}$$

The EKF is efficient for moderately nonlinear systems but may struggle with strong nonlinearities, as the linearization process can introduce approximation errors.

Application of the UKF

The UKF is a nonlinear filtering algorithm designed to estimate the state of a dynamic system. It approximates the state distribution by generating a set of sigma points around the mean state estimate. These sigma points are propagated through the nonlinear system dynamics, allowing the UKF to capture the mean and covariance of the state distribution more accurately than linearization-based methods like the EKF.

Sigma points and weights calculation

The UKF represents the state distribution using a set of carefully chosen sample points, known as sigma points, generated around the current state estimate. These sigma points are then propagated through the nonlinear functions to accurately estimate the mean and covariance of the predicted state.

- Generate sigma points: the sigma points χ are generated as follows:

$$\chi_0 = \hat{\mathbf{x}}_k \tag{34}$$

$$\chi_i = \hat{\mathbf{x}}_k + \gamma\sqrt{\mathbf{P}_k}, \quad \chi_{i+L} = \hat{\mathbf{x}}_k - \gamma\sqrt{\mathbf{P}_k}, \quad i = 1,\ldots,L \tag{35}$$

where $\gamma = \sqrt{L+\lambda}$ is a scaling factor, $\lambda = \alpha^2(L+\kappa) - L$ is a parameter that determines the spread of the sigma points around the mean, L is the dimensionality of the state vector.

- α is a small positive constant (typically 1×10^{-3}), and κ is a secondary scaling parameter, often set to 0.

- Weights for sigma points: each sigma point is assigned a weight for the calculation of the mean and covariance. The weights are computed as follows:

Weight for the mean

$$W_m^{(0)} = \frac{\lambda}{L+\lambda} \tag{36}$$

Weight for the covariance

$$W_c^{(0)} = \frac{\lambda}{L+\lambda} + (1-\alpha^2+\beta) \tag{37}$$

Here, β is a parameter that incorporates prior knowledge of the distribution of the state. For Gaussian distributions, $\beta = 2$ is typically used.

Weights for other sigma points

$$W_m^{(i)} = W_c^{(i)} = \frac{1}{2(L+\lambda)}, \quad \text{for } i = 1,\ldots,2L \tag{38}$$

The UKF algorithm involves two main steps: prediction and update.

Prediction step

- Propagation of sigma points: the sigma points are propagated through the nonlinear state transition function:

$$\chi_{k+1|k}^{(i)} = \boldsymbol{f}(\chi_k^{(i)}) \tag{39}$$

- Mean and covariance estimation: the predicted state mean and covariance are computed using the propagated sigma points:

$$\hat{\mathbf{x}}_{k+1|k} = \sum_{i=0}^{2L} W_m^{(i)} \chi_{k+1|k}^{(i)} \tag{40}$$

$$\mathbf{P}_{k+1|k} = \sum_{i=0}^{2L} W_c^{(i)} \left(\chi_{k+1|k}^{(i)} - \hat{\mathbf{x}}_{k+1|k} \right) \left(\chi_{k+1|k}^{(i)} - \hat{\mathbf{x}}_{k+1|k} \right)^{\mathrm{T}} + \mathbf{Q} \tag{41}$$

Update step

- Transformation of sigma points through measurement function: the sigma points are transformed through the nonlinear measurement function:

$$\boldsymbol{Z}_{k+1}^{(i)} = \boldsymbol{h}(\chi_{k+1|k}^{(i)}) \tag{42}$$

- Measurement mean and covariance: the predicted measurement mean and covariance are calculated:

$$\hat{\mathbf{z}}_{k+1} = \sum_{i=0}^{2L} W_m^{(i)} \mathbf{Z}_{k+1}^{(i)} \tag{43}$$

$$\mathbf{P}_{z_{k+1}} = \sum_{i=0}^{2L} W_c^{(i)} \left(\mathbf{Z}_{k+1}^{(i)} - \hat{\mathbf{z}}_{k+1} \right) \left(\mathbf{Z}_{k+1}^{(i)} - \hat{\mathbf{z}}_{k+1} \right)^{\mathrm{T}} + \mathbf{R} \tag{44}$$

- Cross covariance and Kalman gain: the cross covariance between the state and measurement is computed, and the Kalman gain is obtained:

$$\mathbf{P}_{xz_{k+1}} = \sum_{i=0}^{2L} W_c^{(i)} \left(\chi_{k+1|k}^{(i)} - \hat{\mathbf{x}}_{k+1|k} \right) \left(\mathbf{Z}_{k+1}^{(i)} - \hat{\mathbf{z}}_{k+1} \right)^{\mathrm{T}} \tag{45}$$

$$\mathbf{K}_k = \mathbf{P}_{xz_{k+1}} \mathbf{P}_{z_{k+1}}^{-1} \tag{46}$$

- State and covariance update: the state estimate and covariance are updated using the Kalman gain:

$$\hat{\mathbf{x}}_{k+1} = \hat{\mathbf{x}}_{k+1|k} + \mathbf{K}_k \left(\mathbf{z}_{k+1} - \hat{\mathbf{z}}_{k+1} \right) \tag{47}$$

$$\mathbf{P}_{k+1} = \mathbf{P}_{k+1|k} - \mathbf{K}_k \mathbf{P}_{z_{k+1}} \mathbf{K}_k^T \tag{48}$$

The UKF is particularly effective in providing accurate estimates for highly nonlinear systems, outperforming the EKF by directly addressing the nonlinearities in the state transition and measurement processes without relying on linearization.

Simulation setup

This section simulates the tank dynamics using a second-order Gauss-Markov process and compares the effectiveness of the UKF and the EKF in estimating the tank's states through a single simulation. Additionally, it evaluates the estimation errors of both filters through Monte Carlo simulations. An overview of the simulation setup is provides, including the initial conditions and parameters of the tank's kinematics and dynamics, as well as the configurations of the UKF and EKF used in the study. The simulation is conducted over a 20-second interval with a time step of 0.1 seconds. The tank's true position, velocity, and acceleration are generated using the second-order Gauss-Markov process, and both UKF and EKF are applied to estimate these states based on noisy position measurements. The parameters used for the simulation programs are shown in Tables 1, 2, and 3.

Table 1. Initial conditions and system parameters.

Category	Parameters	Symbol	Values
Simulation setup	Simulation time	T	20 s
	Time step	Δt	0.1 s
	Number of Monte Carlo simulations	N	1,000
System dynamics parameters	Damping coefficient	ζ	0.7
	Natural frequency	ω_n	1.256 rad/s
	Time constant	T	2.6 s
	Magnitude of the process noise affecting the system	σ_W	0.5
Initial state conditions	Initial position of the tank	X_{T0}	0 m
	Initial velocity of the tank	V_{T0}	5 m/s
	Initial acceleration of the tank	a_{Tx0}	1 m/s²
Constraints on motion	Maximum allowable acceleration of the tank	$\|a_{Tx}\|$ max	2 m/s²
	Maximum allowable velocity of the tank	$V_{T\max}$	25 m/s

Source: Elaborated by the authors.

Table 2. UKF parameters.

Parameter	Symbol	Value	Description
State dimension	L	3	Dimension of the state vector (position, velocity, acceleration)
Spread parameter	α	10^{-3}	Determines the spread of the sigma points
Centrality parameter	κ	0	Affects the spread and centrality of the sigma points
Distribution parameter	β	2	Used to incorporate prior knowledge about the distribution (2 for Gaussian)
Lambda	λ	$\alpha^2(L+\kappa)-L$	Calculated parameter for scaling sigma points
Gamma	γ	$\sqrt{L+\lambda}$	Scaling factor for sigma points
Initial covariance matrix	P_{ukf}	0.1* identity matrix (3 × 3)	Initial uncertainty in the state estimate
Process noise covariance matrix	Q	Diagonal matrix with elements (0.01, 0.01, 0.1)	Represents the process noise affecting the system
Measurement noise covariance matrix	R	0.01	Represents the measurement noise affecting the observations

Source: Elaborated by the authors.

Table 3. EKF Parameters

Parameter	Symbol	Value	Description
Initial covariance matrix	P_{ukf}	0.1* identity matrix (3 × 3)	Initial uncertainty in the state estimate
Process noise covariance matrix	Q	Diagonal matrix with elements (0.01, 0.01, 0.1)	Represents the process noise affecting the system
Measurement noise covariance matrix	R	0.01	Represents the measurement noise affecting the observations

Source: Elaborated by the authors.

Initial conditions and parameters

The tank's true position, velocity, and acceleration are generated using a second-order Gauss-Markov process, as described in the section "Nonlinear state transition function and measurement function".

This section outlines the configuration of the two filters – UKF and EKF – used to estimate the tank's position, velocity, and acceleration.

The UKF and EKF are both initialized with identical initial state estimates of (0; 0; 0), representing the starting assumptions for position, velocity, and acceleration. This ensures a fair comparison between the two filters.

Simulation framework for comparing UKF and EKF in nonlinear target tracking

This section presents simulations conducted to evaluate the performance of different filtering techniques in estimating the tank's dynamics. The analysis focuses on the following key aspects:

- Tank dynamics simulation using a second-order Gauss-Markov process: the tank's position, velocity, and acceleration are simulated over time using a second-order Gauss-Markov process, incorporating complex dynamic factors such as damping, natural frequency, and the influence of random noise to realistically replicate operational conditions.
- Comparison of UKF and EKF Performance in estimating tank states: the performance of the UKF and the EKF is evaluated through a single simulation, focusing on their ability to estimate the tank's states accurately in comparison to the true states generated by the simulation.
- Evaluation of UKF and EKF estimation errors through Monte Carlo simulations: this expands the analysis by comparing the accuracy of UKF and EKF across multiple simulations, providing a statistical perspective on their estimation errors.

By integrating these components, the section provides a comprehensive analysis of the tank's behavior and the strengths and weaknesses of the UKF and EKF filters. The results highlight the effectiveness of the second-order Gauss-Markov process in simulating realistic tank dynamics while identifying the scenarios where each filtering approach performs optimally. This foundation supports further development and application of advanced state estimation techniques in nonlinear systems.

Figure 2 presents a flowchart of the algorithm for evaluating the estimation error of UKF and EKF through Monte Carlo simulation, providing an overview of the entire simulation process. Since this flowchart already covers all the necessary information, detailed flowcharts for individual subprocesses, such as modeling the position, velocity, and acceleration of the tank according to a second-order Gauss-Markov process, or comparing UKF and EKF in estimating the tank dynamics through a single simulation with random states, will be omitted as they have already been integrated into this general flowchart.

RESULTS AND DISCUSSION

Simulation of tank dynamics using a second-order Gauss-Markov process

The purpose of the simulation of tank dynamics using a second-order Gauss-Markov process is to model the position, velocity, and acceleration of a tank over time, considering the effects of damping and random noise. This simulation provides insights into how the tank's dynamics evolve under these influences, resulting in time-based plots of the tank's position, velocity, and acceleration. These results are crucial for understanding the tank's behavior in realistic operational conditions, helping to inform the design and testing of control and estimation algorithms.

Figure 3 illustrates the tank dynamics simulated using a second-order Gauss-Markov process. The plots display the position, velocity, and acceleration of the tank over the 20-second simulation period. The second-order Gauss-Markov process successfully captures the oscillatory and damping behavior characteristic of the tank's movement: (a) Position; (b) Velocity; (c) Acceleration.

The tank's acceleration plot reveals the system's characteristic oscillation, reflecting the impact of random variations in the second-order Gauss-Markov model. Each simulation generates a distinct motion scenario for the tank, highlighting the randomness of its movement under real-world conditions. These results are crucial as input data for evaluating the reliability of guidance algorithms and the accuracy of state estimation filters applied to the tank dynamics model. Furthermore, they confirm the model's effectiveness in accurately simulating the tank's motion, laying the groundwork for a detailed comparison between the UKF and EKF methods.

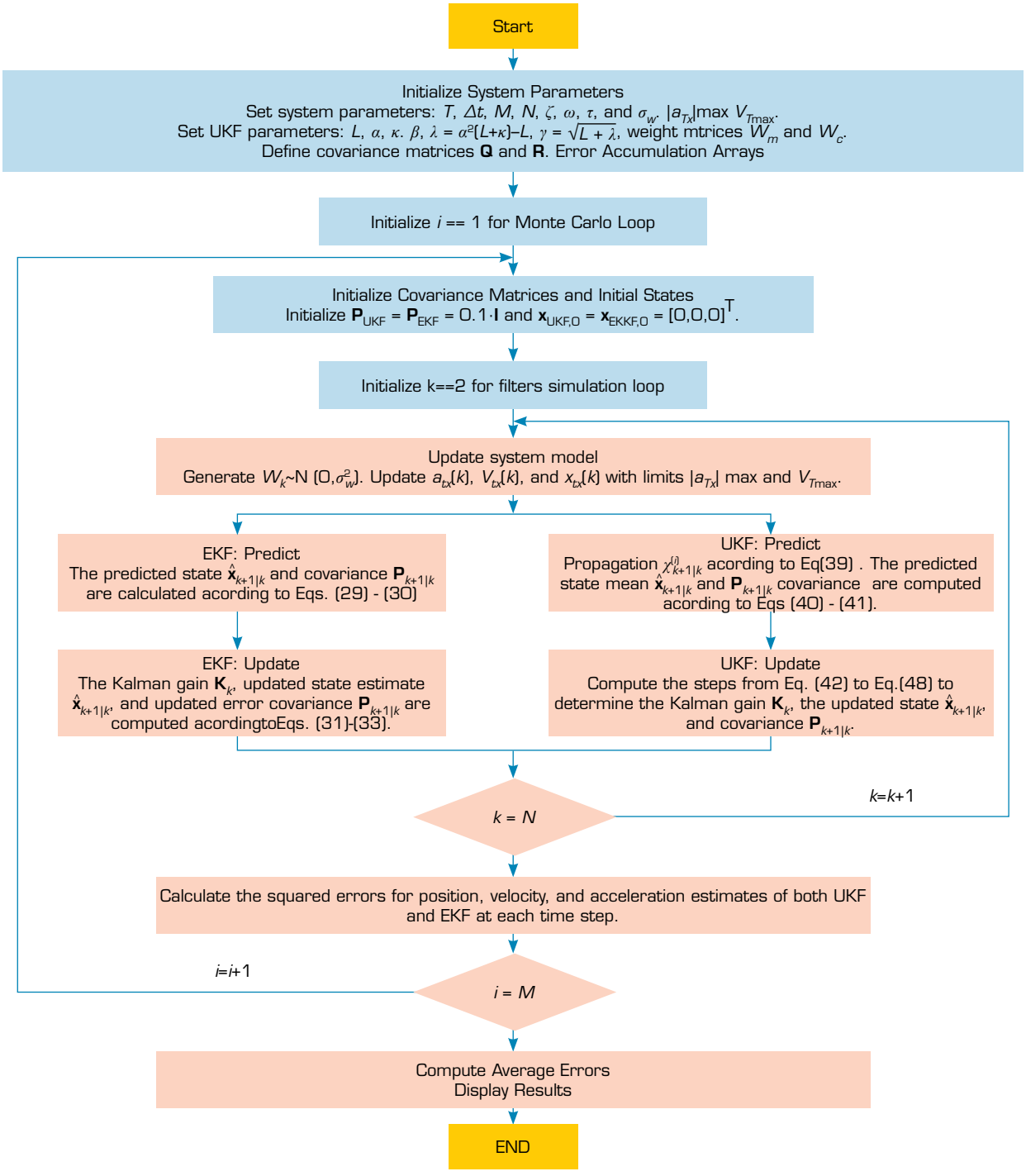

Source: Elaborated by the authors.

Figure 2. Algorithm flowchart for Monte Carlo simulation assessing the performance of UKF and EKF filters.

Comparison of UKF and EKF in estimating tank dynamics through a single simulation

In this approach, a single simulation run is conducted to compare the performance of the UKF and the EKF in estimating the position, velocity, and acceleration of a moving tank. The tank's dynamics are simulated using a second-order Gauss-Markov process, which includes nonlinearities and random noise.

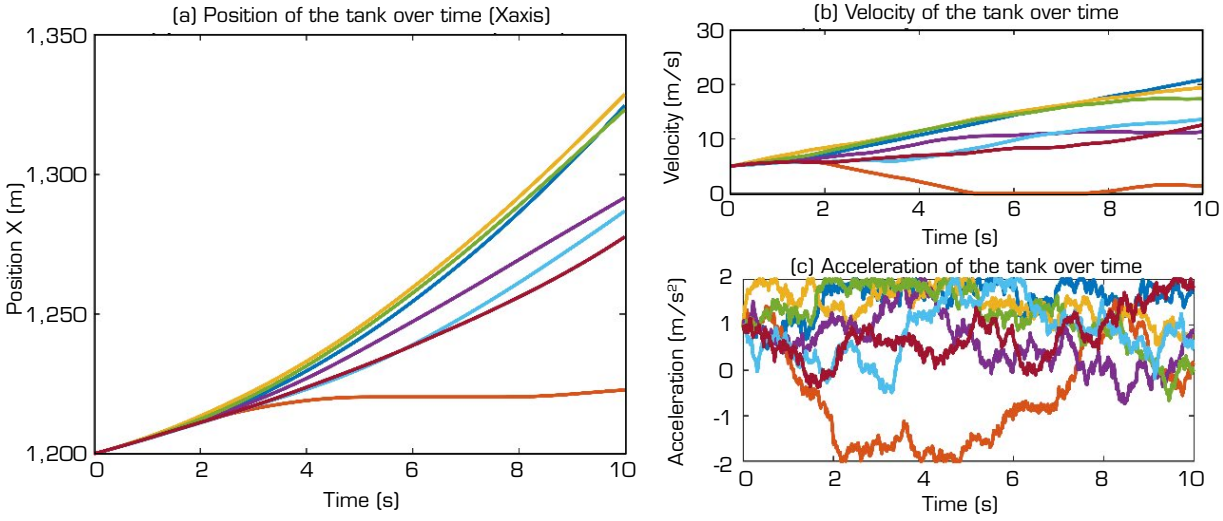

Source: Elaborated by the authors.

Figure 3. Simulation of tank dynamics using a second-order Gauss-Markov process.

Purpose of the comparison

The main objective is to observe and compare the accuracy of the estimates from UKF and EKF in real time by directly comparing the estimated states (position, velocity, acceleration) of both filters with the actual values generated in the simulation. Conducting just one simulation run provides a quick and visual comparison of the performance of the two filters, although it does not offer comprehensive statistical insight.

Figure 4 presents a direct comparison between the UKF and EKF in estimating the tank's position, velocity, and acceleration. The plots demonstrate that the UKF provides more accurate estimates compared to the EKF, particularly under nonlinear and noisy conditions. The UKF's ability to handle nonlinear models without linearization results in lower estimation errors, which is clearly evident in the velocity and acceleration plots. In contrast, the EKF, which relies on linear approximations, shows greater

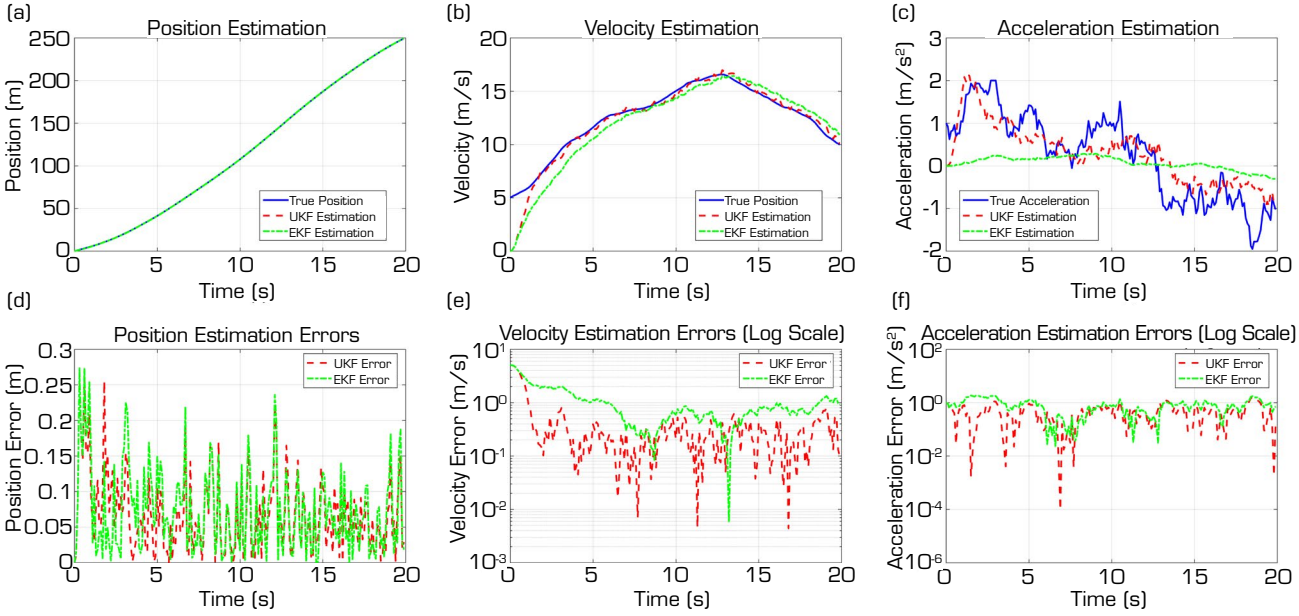

Source: Elaborated by the authors.

Figure 4. Comparison of tank position, velocity, and acceleration estimates between UKF and EKF with actual values.

deviations from the true values, especially during rapid changes in acceleration. These findings highlight the superiority of the UKF in handling the complex nonlinear dynamics of the tank.

Evaluation of estimation errors in UKF and EKF using Monte Carlo simulation

The tank system's dynamic state is simulated using a second-order Gauss-Markov process, resulting in different outcomes for each simulation run. Therefore, the Monte Carlo method is applied with 1,000 simulation runs to calculate the average estimation errors for each state (position, velocity, acceleration) of the tank. This method provides a comprehensive view of the accuracy and reliability of the filters (UKF and EKF) when handling random variations in real-world conditions.

This comparison evaluates the performance of the two filters in complex nonlinear systems and identifies the filter better suited for tracking maneuvering targets, such as a tank in combat scenarios.

Assume $\hat{\mathbf{x}}_i(t)$ represents the estimated target parameters (position, velocity, and acceleration) output by the UKF and EKF filters in the i-th run at time i. The Monte Carlo average of the estimation error at time t can be calculated as follows:

$$\overline{e}(t) = \frac{1}{M}\sum_{i=1}^{M} e_i(t) \tag{49}$$

where M is the total number of trials (here, 1,000 runs), $\mathbf{e}_i(t) = \hat{\mathbf{x}}_i(t) - \mathbf{x}_{\text{true}}(t)$ is the estimation error for the i-th run at time t, and $\mathbf{x}_{\text{true}}(t)$ is the true value of the target parameters at time t. The value $\overline{e}(t)$ reflects the average deviation from the true value over 1,000 runs at time t, providing insight into the effectiveness of the UKF and EKF in estimating the target state.

Figure 5 illustrates the estimation errors of the UKF and EKF across multiple Monte Carlo simulation runs. The plots show that, on average, the UKF consistently outperforms the EKF in terms of lower estimation errors for position, velocity, and acceleration. The histogram charts of the errors indicate that the UKF not only has a lower mean error but also exhibits less variability in its estimates compared to the EKF. This is particularly evident in scenarios with high levels of process noise, where the linearization approach of the EKF fails to accurately track the tank's states.

These results reinforce the advantage of the UKF in scenarios where the system dynamics are highly nonlinear and affected by significant uncertainties. The simulation results clearly demonstrate that the UKF outperforms the EKF in estimating the dynamic states of a maneuvering tank, particularly in environments with nonlinear dynamics and uncertain noise. The improved performance of the UKF is attributed to its ability to handle nonlinear models more effectively, as evidenced by lower estimation errors in both single simulations and Monte Carlo trials.

These findings suggest that the UKF is a more suitable choice for applications involving complex nonlinear systems, such as military vehicle tracking, where accurate state estimation is crucial.

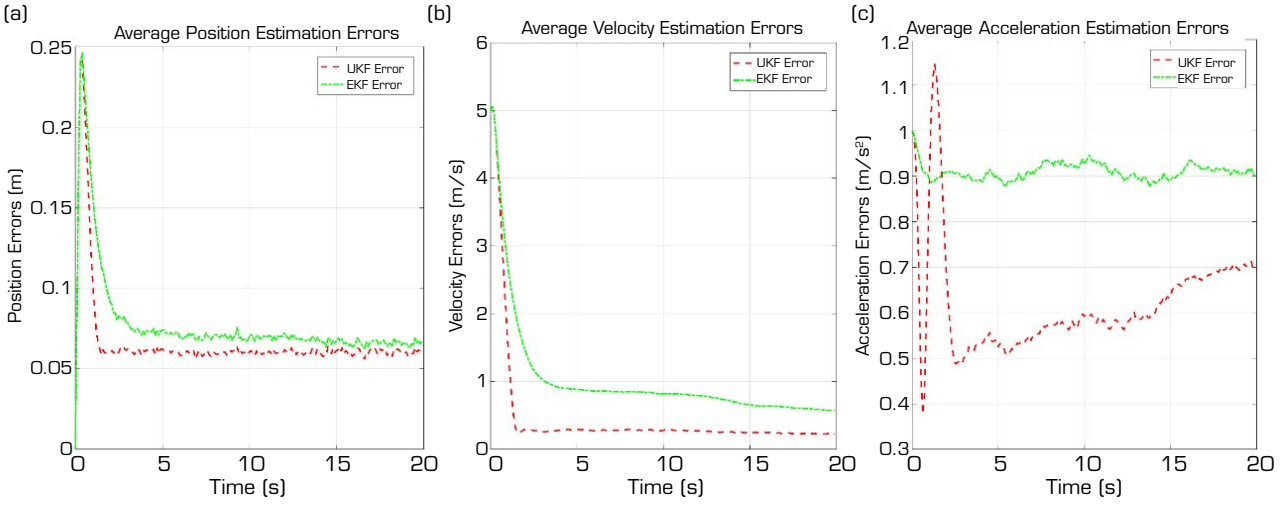

Source: Elaborated by the authors.

Figure 5. Monte Carlo simulation result.

CONCLUSION

This study has demonstrated the effectiveness of using a second-order Gauss-Markov process to model the dynamic states of a maneuvering tank, capturing the inherent oscillatory and damping characteristics of such systems. The UKF, applied to this advanced modeling framework, has proven superior to the EKF in estimating the tank's position, velocity, and acceleration.

The UKF's ability to handle nonlinearities without requiring linearization provided a significant advantage, as demonstrated by more accurate and stable estimates. The Monte Carlo simulations further reinforced the superiority of the UKF, showing lower estimation errors and less variability compared to the EKF.

These results underscore the importance of advanced modeling and estimation techniques for accurate state tracking in complex real-world applications. Future work could involve extending the study to more complex scenarios, such as multi-target tracking and the inclusion of more sophisticated tank maneuvers. Additionally, integrating the UKF with other sensor fusion techniques could further enhance tracking accuracy and performance.

CONFLIT OF INTEREST

Nothing to declare.

AUTHORS' CONTRIBUTION

Conceptualization: Van HT; **Methodology:** Ngoc DN, Trung DP; **Validation:** Trung DP; **Writing - Original draft:** Van HT; **Writing -Review & editing:** Van HT and Duy PN; **Final approval:** Van HT.

DATA AVAILABILITY STATEMENT

All data sets were generated or analyzed in the current study.

FUNDING

Not applicable.

ACKNOWLEDGEMENTS

Not applicable.

REFERENCES

Bellar A (2019) Satellite inertia parameters estimation based on extended Kalman filter. J Aerosp Technol Manag 11. Available at https://www.scielo.br/j/jatm/a/9GvJDNcXDyz6D43HCmFDcXp/abstract/?lang=en

Chen Y, Jilkov V, Li X (2015) Multilane-road target tracking using radar and image sensors. IEEE Trans Aerosp Electron Syst 51:65-80. https://doi.org/10.1109/TAES.2014.120766

Chen X, Yaan L, Li Y, Yu J (2017) PHD and CPHD algorithms based on a novel detection probability applied in an active sonar tracking system. Appl Sci 8:36. https://doi.org/10.3390/app8010036

Ebrahimi M, Ardeshiri M, Khanghah SA (2022) Bearing-only 2D maneuvering target tracking using smart interacting multiple model filter. Digit Signal Process 126:103497. https://doi.org/10.1016/j.dsp.2022.103497

Gibbs BP (2011) Modeling examples. Advanced Kalman filtering, least-squares and modeling. New Jersey: John Wiley & Sons.

Gite LK, Deodhar RS (2022) Estimation of yaw angle from flight data using extended Kalman filter. Aerosp Sci 5(3):393-402. https://doi.org/10.1007/s42401-022-00131-3

Jagan B, Koteswara RS, Jahan K (2021) Unscented particle filter approach for underwater target tracking. Int J e-Collab 17:29. https://doi.org/10.4018/IJeC.2021100103

Kaur N, Kaur A (2016) Tuning of extended Kalman filter for nonlinear state estimation. IOSR J Comput Eng 18:14-19. https://doi.org/10.9790/0661-1805041419

Li XR, Jilkov VP (2003) Survey of maneuvering target tracking. Part I. Dynamic models. IEEE Trans Aerosp Electron Syst 39(4):1333-1364. https://doi.org/10.1109/TAES.2003.1261132

Masooleh LS, Arbogast JE, Seider WD, Oktem U, Soroush M (2022) Distributed state estimation in large-scale processes decomposed into observable subsystems using community detection. Comput Chem Eng 156:107544. https://doi.org/10.1016/j.compchemeng.2021.107544

Ponsa D, Lopez A, Serrat J, Lumbreras F, Graf T (2005) Multiple vehicle 3D tracking using an unscented Kalman. Paper presented 2005 IEEE Intelligent Transportation Systems. IEEE; Vienna, Austria. https://doi.org/10.1109/ITSC.2005.1520206.

Rao SK, Babu VS (2008) Unscented Kalman filter with application to bearings-only passive maneuvering target tracking. Paper presented 2008 International Conference on Signal Processing, Communications and Networking. Event Organizer; Chennai, India. https://doi.org/10.1109/ICSCN.2008.4447192

Sreeja S, Hablani HB (2016) Precision munition guidance and moving-target estimation. J Guid Control Dyn 39(9):2100-2111. https://doi.org/10.2514/1.G000382

Sun M, Ma Z, Li Y (2015) Maneuvering target tracking using IMM Kalman filter aided by Elman neural network. Paper presented 2015 7th International Conference on Intelligent Human-Machine Systems and Cybernetics. Event Organizer; City, Country.

Van DNNHT, Trung DP, Nguyen TT (2024) Nonlinear guidance laws for anti-tank guided missile to intercept maneuvering tank targets using optimal error dynamics and relative virtual model. J Aerosp Technol Manag 16. https://doi.org/10.1590/jatm.v16.1344

Visina R, Bar-Shalom Y, Willett P (2018) Multiple-model estimators for tracking sharply maneuvering ground targets. IEEE Trans Aerosp Electron Syst 54(3):1404-1414. https://doi.org/10.1109/TAES.2018.2793019

Wan EA, Merwe RVD (2000) The unscented Kalman filter for nonlinear estimation. Paper presented 2000 IEEE daptive Systems for Signal Processing, Communications, and Control Symposium. IEEE; Louise, Canada. https://doi.org/10.1109/ASSPCC.2000.882463.

Zhai G, Wu C, Wang Y (2018) Millimeter wave radar target tracking based on adaptive Kalman filter. Paper presented 2018 IEEE Intelligent Vehicles Symposium. IEEE; Changshu, China. http://dx.doi.org/10.1109/IVS.2018.8500505

Zhang A, Bao S, Gao F, Wenhao B (2019) A novel strong tracking cubature Kalman filter and its application in maneuvering target tracking. Chinese J Aeronaut 32. https://doi.org/10.1016/j.cja.2019.07.025